Physica E 131 (2021) 114736

Contents lists available at ScienceDirect

Physica E: Low-dimensional Systems and Nanostructures

journal homepage: http://www.elsevier.com/locate/physe

First principle study of transition metals codoped MoS_2 as a gas sensor for the detection of NO and NO_2 gases

Ehab Salih [a], Ahmad I. Ayesh [a,b,*]

[a] Department of Mathematics, Statistics and Physics, Qatar University, P. O. Box 2713, Doha, Qatar
[b] Center for Sustainable Development, Qatar University, P. O. Box 2713, Doha, Qatar

ARTICLE INFO

Keywords:
MoS_2
Gas adsorption
Codoping
Gas sensor
DFT

ABSTRACT

Exposure to nitrogen oxides (NO_x) has been reported to seriously affect the respiratory systems. More precisely, breathing NO_x may lead to the appearance of asthma symptoms, and may also result in the infection with asthma over long intervals. This study is devoted to finding novel systems to detect nitric oxide (NO) and nitrogen dioxide (NO_2) with improved sensitivity. Consequently, gold (Au) and silver (Ag) codoped molybdenum disulfide (MoS_2) (Au–Ag–MoS_2) is proposed as NO and NO_2 gas sensor based on density functional theory (DFT) calculations. The variations of the electronic properties as well as the adsorption parameters of the new proposed sensor upon the adsorption of NO and NO_2 gases are compared with pristine, Au-doped, and Ag-doped MoS_2. The results reflect a remarkable change in the band gap of the developed systems upon the adsorption of NO and NO_2 gases. Meanwhile, the adsorption parameters demonstrate that the Au doped MoS_2 system is selective to NO, while the codoped MoS_2 system is selective to NO_2. Specifically, the Au-doped MoS_2 exhibits its maximum adsorption energy (E_{ads}) towards NO of −0.721 eV. Moreover, the highest adsorption energy and charge transfer (ΔQ) are found to be −2.603 eV and 0.448 e, respectively, for the case of NO_2/Au–Ag-codoped MoS_2. Hence, our investigation suggests that Au–Ag-codoped MoS_2 can be utilized as a gas sensor for the detection of NO_2 gas.

1. Introduction

The need for an effective gas sensor for the purpose of monitoring the level of nitrogen oxides (NO_x) is growing not only for industrial applications but also in medicine [1]. Sensing the molecules of NO gas, for example, in the exhaled breath is utilized in predicting the infection with asthma and some other respiratory diseases [2,3]. Specifically, if the concentration is above 50 ppb, this can be considered as an indication of inflammation in the airways [3,4]. Furthermore, NO gas can be easily transformed, via oxidation, to the more poisonous nitrogen dioxide gas (NO_2) [5,6]. NO_2 is a poisonous gas generated mainly through fuel combustion in industry and automotive emissions [7]. In addition to being one of the common air pollutants, NO_2 could facilitate the infection of various diseases not only at high concentrations but at low concentrations as well [8]. Accordingly, the early and sensitive detection of NO_x gases at low concentrations is of great importance to human beings.

Two-dimensional nanomaterials (2D-NMs) including graphene as well as transition metal dichalcogenides (TMDs) have been extensively studied, thanks to their outstanding performance in different applications, as a result of their large surface areas as well as the plenty of active sites [9,10]. Among the TMDs, considerable interest has been directed to molybdenum disulfide (MoS_2) monolayer in the field of sensors due to its superior chemical, physical, and electrical characteristics [11–14]. MoS_2 monolayer is a direct band gap semiconductor that consists of a layer of Mo atoms between two lower and upper layers of S atoms producing a sandwiched material [15–17]. Each Mo atom in the MoS_2 monolayer is bonded covalently to six S atoms forming 2D crystal [17,18].

Pham et al. investigated the bandgap of chemical vapor deposition fabricated mono-layer of MoS_2 with Au, and then applied for NO_2 gas sensing. The results reveal significant improvement of the MoS_2 sensitivity for low level of NO_2 gas. The detection limit for NO_2 gas was 0.1 ppb for the Au modified MoS_2 [19]. Ma et al. studied the adsorption of both CO and NO gases on MoS_2 monolayers modified with Au, Pt, Pd, or Ni. They found that charge transfer among MoS_2 and the adsorbed molecules for both gases. The adsorption of NO induces impurity states and their effects are observed in the band gap as redistribution of states. Furthermore, NO adsorption leads to variation of transport properties of MoS_2 [20].

* Corresponding author. Department of Mathematics, Statistics and Physics, Qatar University, P. O. Box 2713, Doha, Qatar.
E-mail address: ayesh@qu.edu.qa (A.I. Ayesh).

https://doi.org/10.1016/j.physe.2021.114736
Received 6 February 2021; Received in revised form 26 February 2021; Accepted 17 March 2021
Available online 19 March 2021

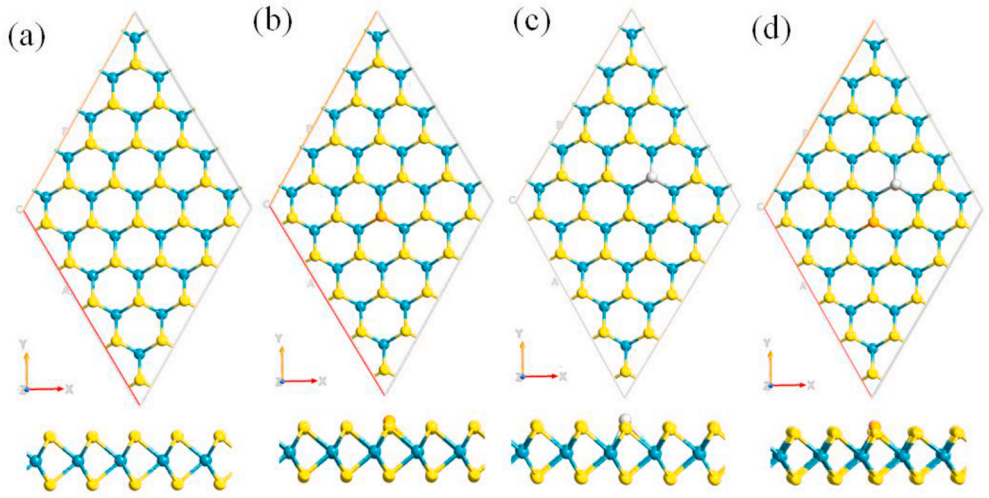

Fig. 1. Top and side views of a) MoS_2, b) Au–MoS_2, c) Ag–MoS_2, and d) Au–Ag–MoS_2.

Table 1
Geometrical parameters of MoS_2, Au–MoS_2, Ag–MoS_2, and Au–Ag–MoS_2.

System	Bond length (Å)		
	Mo–S	Mo–Au	Mo–Ag
MoS_2	2.420	–	–
Au–MoS_2	2.410*	2.740	–
Ag–MoS_2	2.415*	–	2.810
Au–Ag–MoS_2	2.408*	2.753	2.803

Herein, the influence of doping and codoping by transition metal (Au and Ag) of MoS_2 on the electronic features and the adsorption capability toward NO_x gases is investigated computationally based on density functional theory (DFT). The results demonstrated considerable variations in the electronic properties of MoS_2 upon doping with Au and Ag and codoping with both atoms. Furthermore, a remarkable enhancement in the adsorption parameters is noticed for the cases of Au–MoS_2, Ag–MoS_2 and Au–Ag–MoS_2 systems when compared with the pristine MoS_2. Consequently, codoping of MoS_2 with transition metals can be recommended as an effective method of improving its performance for gas sensing.

2. Computational details

Atomistic ToolKit Virtual NanoLab (ATK-VNL) based on DFT method was used to investigate the electronic properties as well as the sensing capability of MoS_2 based sensor materials. More precisely, a (5 × 5) supercell of MoS_2 monolayer has been built as a substrate, and a central S atom was substituted by a transition metal atom (Au and Ag) generating two doped systems: Au–MoS_2 and Ag–MoS_2. Codoping was also utilized to generate the system: Au–Ag–MoS_2. The generalized gradient approximation (GGA) was engaged with the Perdew-Burke-Ernzerhof (PBE) for defining the electron exchange and correlation [21,22]. Meanwhile, DFT-D2 of Grimme was implemented in order to correct the impact of Van der Waals interactions [22]. During all the calculations, we selected the energy mesh cutoff, force tolerance, and stress error tolerance as 100 Ry, 0.05 eV/Å, and 0.1 GPa, respectively. For Brillouin-zone sampling, a 5 × 5 × 1 k-point sample of Monkhorst-Pack grid has been utilized for the geometry optimization along with the electronic properties investigations.

To evaluate the adsorption of NO and NO_2 gases on any of the proposed MoS_2, Au– MoS_2, Ag– MoS_2, and Au–Ag– MoS_2 sensors, the adsorption energy has been calculated by utilizing Equation (1)

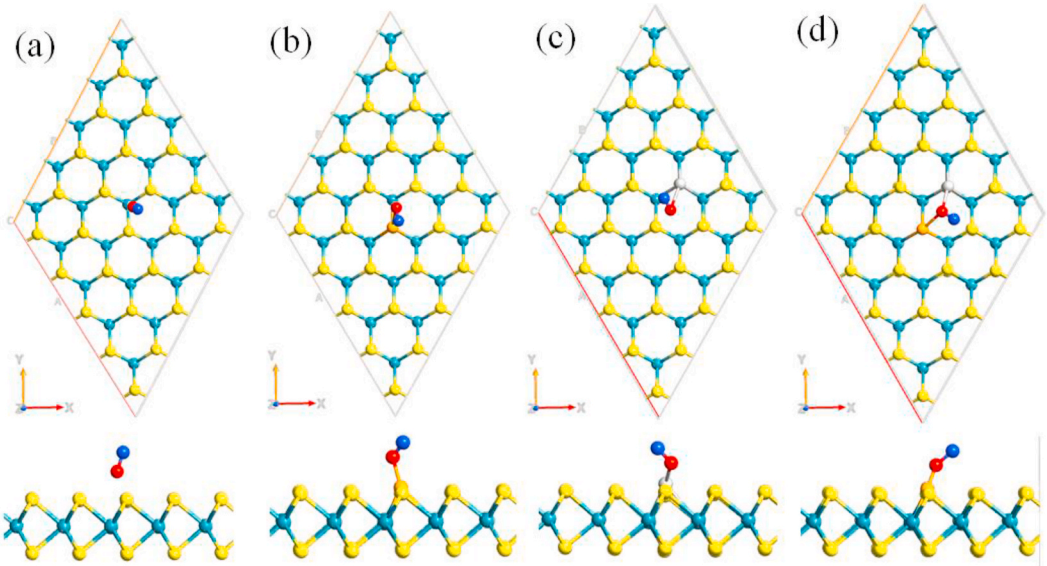

Fig. 2. Top and side views of a) NO/MoS_2, b) NO/Au–MoS_2, c) NO/Ag–MoS_2, and d) NO/Au–Ag–MoS_2.

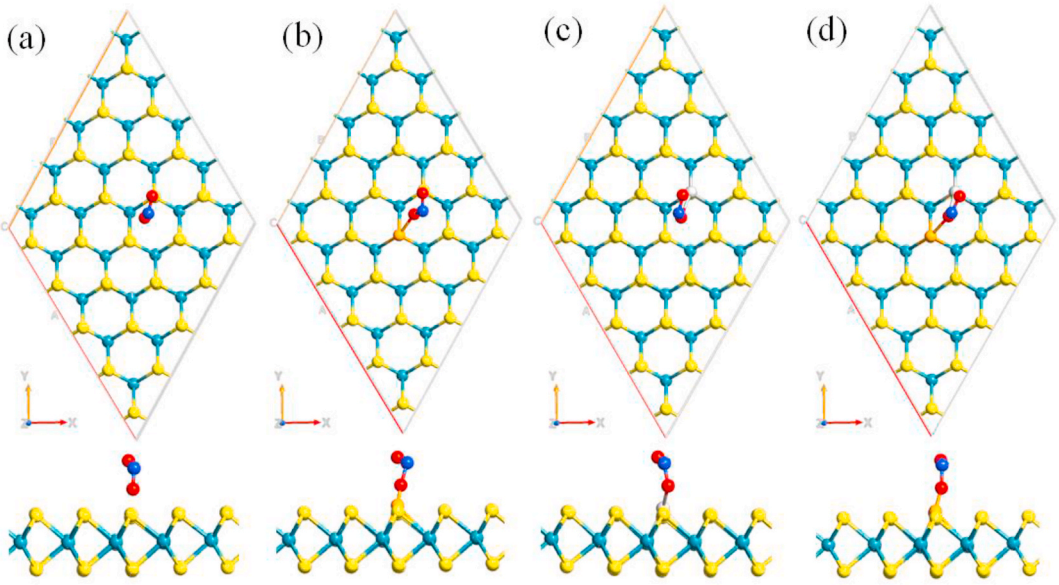

Fig. 3. Top and side views of a) NO_2/MoS_2, b) NO_2/Au–MoS_2, c) NO_2/Ag–MoS_2, and d) NO_2/Au–Ag–MoS_2.

Table 2
Adsorption energy and distance along with charge transfer of the developed adsorption systems.

System	Adsorption Energy (eV)	Adsorption Length (Å)	Charge Transfer (e)
NO/MoS_2	0.107	2.45	−0.047
NO/Au–MoS_2	−0.721	2.16	0.113
NO/Ag–MoS_2	−0.384	2.18	0.133
NO/ Au–Ag–MoS_2	−0.553	2.17	0.220
NO_2/MoS_2	−0.155	2.23	0.131
NO_2/Au–MoS_2	−1.596	2.08	0.423
NO_2/Ag–MoS_2	−1.850	2.18	0.442
NO_2/ Au–Ag–MoS_2	−2.603	2.19	0.448

[23–25]:

$$E_{ads} = E_{Au/Ag-MoS_2+NO_x} - E_{Au/Ag-MoS_2} - E_{NO_x} \quad (1)$$

Where $E_{Au-Ag-MoS_2+NO_x}$ represents the total energy of either of NO_x/MoS_2, NO_x/Au– MoS_2, NO_x/Ag– MoS_2, or NO_x/Au–Ag– MoS_2 systems, $E_{Au/Ag-MoS_2}$ refers to the total energy of either of developed four sensors without NO_x, and E_{NO_x} – refers to the total energy of either NO or NO_2 gas. Meanwhile, to further confirm the adsorption of NO and NO_2 molecules on the proposed sensor materials, the transfer of charge between the gases and the sensors was calculated based on Mulliken population method by utilizing Equation (2) [24,26]:

$$\Delta Q = Q_a - Q_p \quad (2)$$

Where, ΔQ refers to the net charge transfer of any of the NO and NO_2 gases, Q_a is the Mulliken charges of any of the NO or NO_2 molecules after adsorption on either of the proposed sensors, and Q_p refers to the Mulliken charge of the pure NO or NO_2 gas.

3. Results and discussion

In the present investigation, MoS_2 is chosen as the substrate for the development of a highly sensitive gas sensor for the detection of NO and NO_2 gases. In order to enhance the sensing performance of MoS_2, it's firstly doped with either of Au or Ag atom, and then codoped with both of them. The optimized structures of MoS_2, Au–MoS_2, Ag–MoS_2, and Au–Ag–MoS_2 systems are shown in Fig. 1. Additionally, the geometrical parameters are presented in Table 1. The results reveal that the average Mo–S bond length is 2.420 Å for the case of MoS_2. While for the cases of Au–MoS_2 and Ag–MoS_2, the average Mo–Au and Mo–Ag are 2.740 Å and 2.810 Å, respectively. Meanwhile, the length of Mo–S bonds close to the position of substitution with Au and Ag changes a little to 2.410 Å, and 2.415 Å, respectively. On the other hand, the average Mo–Ag and Mo–Au bond lengths vary a little to 2.753 Å, and 2.803 Å for the case of Au and Ag codoped MoS_2 as shown in Table 1. Fig. 2 shows the optimized NO/MoS_2, NO/Au–MoS_2, NO/Ag–MoS_2, and NO/Au–Ag–MoS_2 systems. As indicated, a chemical bond occurs between the O atom of NO and Au of Au–MoS_2 with a length of 2.16 Å. As a result, the average Mo–Au bond length decreases to 2.69 Å. The same behavior is almost observed for the case of Ag–MoS_2 with an O–Ag bond with a length of 2.18 Å. Furthermore, two bonds are observed between O and both of Au and Ag with lengths of 2.17 and 2.21 Å, respectively, for the case of Au–Ag–MoS_2. The optimized structures of NO_2/MoS_2, NO_2/Au–MoS_2, NO_2/Ag–MoS_2, and NO_2/Au–Ag–MoS_2 systems are shown in Fig. 3. A chemical bond is also observed between one O atom of NO_2 and the doped metals in the cases of Au–MoS_2, Ag–MoS_2, and Au–Ag–MoS_2 verifying the occurrence of strong adsorption. Contrary, no bonds are detected between pristine MoS_2 and the two gases, which justifies the necessity of doping and codoping MoS_2 to improve the adsorption capability.

To confirm the desirable detection of both NO and NO_2 molecules on the developed MoS_2, Au–MoS_2, Ag–MoS_2, and Au–Ag–MoS_2 systems, the adsorption energy E_{ads}, adsorption length l, and the charge transfer ΔQ are calculated. As shown in Table 2, the adsorption energy along with charge transfer are 0.107 eV and −0.047 e for the case of NO/MoS_2, whereas −0.155 eV and 0.131 e for the case of NO_2/MoS_2. Moreover, the adsorption length between the NO and NO_2 gases and MOS_2 are 2.45 and 2.23 Å, respectively. Upon modifying the pristine MoS_2, a remarkable increase in the adsorption energy along with the charge transfer are demonstrated. For instance, the greatest adsorption energy and smallest adsorption length among the three modified systems, for the case of NO gas, are found to be −0.721 eV and 2.16 Å for the case of NO/Au–MoS_2 system. Whereas the highest charge transfer is found to be 0.220 e for the case of NO/Au–Ag–MoS_2. On the other hand, a magnificent increase in the adsorption parameters are detected for the cases of NO_2/Au–MoS_2 NO_2/Ag–MoS_2, and NO_2/Au–Ag–MoS_2 when compared with NO_2/

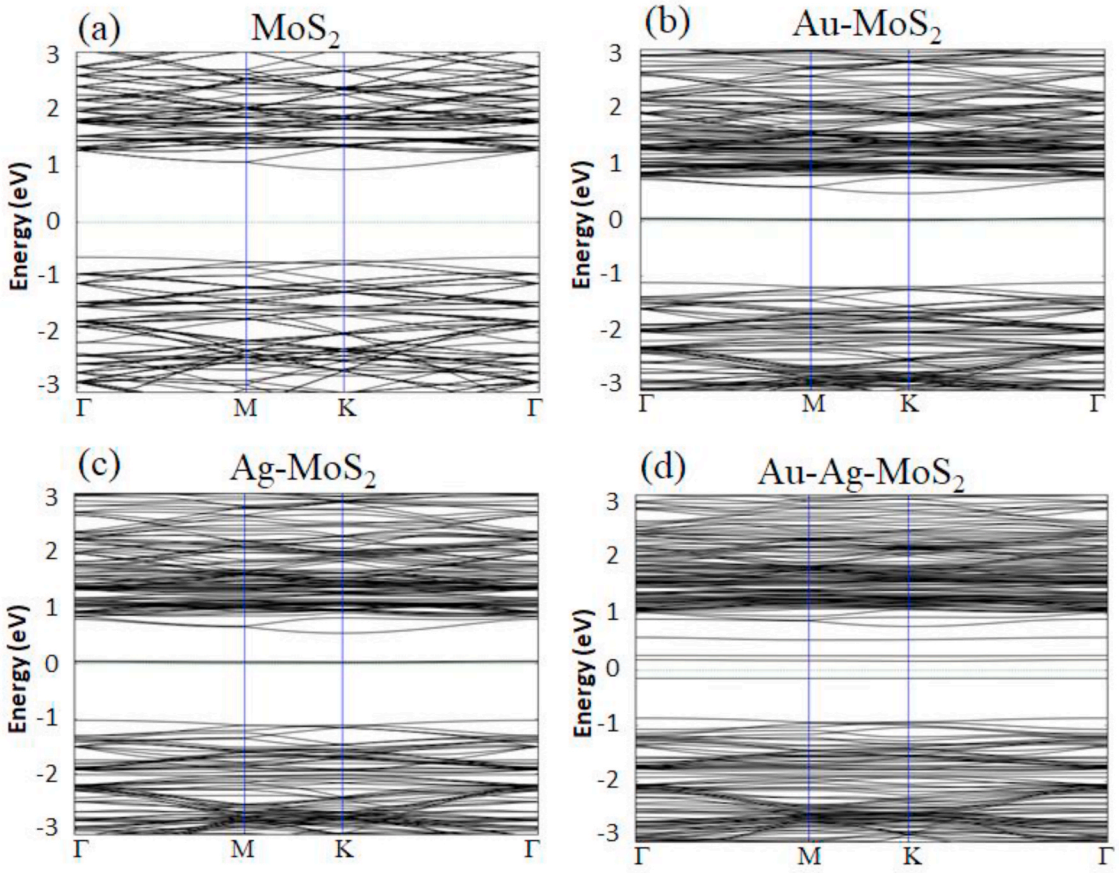

Fig. 4. Band structures of a) MoS_2, b) Au–MoS_2, c) Ag–MoS_2, and d) Au–Ag–MoS_2.

MoS_2. Specifically, the adsorption energy increases to nearly ten times and eleven times for the cases of NO_2/Au–MoS_2, and NO_2/Ag–MoS_2. The smallest adsorption length is observed between NO_2 and Au–MoS_2 system with 2.08 Å. Moreover, the adsorption energy for the case of NO_2/Au–Ag–MoS_2 system increases to almost 16 times, which justifies the importance of codoping MoS_2 with Au and Ag for the purpose of improving the sensing performance. The charge transfer results show that 0.423, 0.442, and 0.448 e transfer from the Au–MoS_2, Ag–MoS_2, and Au–Ag–MoS_2 systems to NO_2 gas, respectively, in the adsorption process. The adsorption parameters obtained in the current study indicate that among the four systems the Au doped MoS_2 system is selective to NO since it exhibits the highest adsorption energy towards NO. Moreover, the newly developed Au–Ag codoped-MoS_2 is selective to NO_2 gas since it exhibits the highest adsorption energy towards NO_2. Additionally, the results also demonstrate that the adsorption of NO and NO_2 molecules on the pristine MoS_2 is physisorption, whereas it is chemisorption for the doped and codoped systems [27–29]. The outstanding improvement in the adsorption capability and hence the sensitivity that is obtained in the current study is attributed to the substitution of S atoms with the transition metals Au and Ag. Such substitution is reported to significantly promote the sensitivity of MoS_2 monolayer toward gas molecules [30,31]. The doped atoms can modify the electronic characteristics of the host material as well as improve the orbital interaction with the target molecules close to the location of substitution [32,33].

The band structures of MoS_2, Au–MoS_2, Ag–MoS_2, and Au–Ag–MoS_2 systems are investigated for a better understanding of the influence of doping as well as codoping MoS_2 monolayer on the electronic properties as presented in Fig. 4. The results show a direct band gap of 1.645 eV for the case of the pure MoS_2 (Fig. 4(a)) which is nearly the same as the experimental value of 1.69 eV [34] as well as the theoretical value of 1.80 eV [35] that have been reported. These results verify the direct band gap semiconductor nature of MoS_2 monolayer [36]. Upon substituting one of the S atoms of MoS_2 with Au and Ag atoms (Fig. 4 (b)-4(c)), the band gap decreases to 1.150 and 1.066 eV, respectively. Meanwhile, the band gap decreases significantly to 0.308 eV after codoping the monolayer of MoS_2 with both Au and Ag as shown in Fig. 4 (c). Additionally, the impact of the gas adsorption on the electronic properties of the developed systems is also investigated as shown in Figs. 7 and 8. Remarkable variations on the electronic features of the modified systems are observed upon the adsorption of NO as well as NO_2 gases. For instance, the band gap significantly decreases to 0.119, 0.145, and 0 eV after the adsorption of NO on Au–MoS_2, Ag–MoS_2, and Au–Ag–MoS_2, respectively. Meanwhile, the band gaps of NO_2/Au–MoS_2, NO_2/Ag–MoS_2, and NO_2/Au–Ag–MoS_2 systems are 0.707, 0.638, and 0 eV, respectively, reflecting a decrease upon the gas adsorption. Furthermore, some new bands are observed in the valence and conduction bands after modifying MoS_2 as well as the adsorption of the two gases. These variations in the electronic features is a justification of the origination of new electronic states thanks to the adsorption of NO and NO_2 molecules [37].

The results obtained from the band structures are further examined with the density of states investigations. The density of state of pristine MoS_2, Au–MoS_2, Ag–MoS_2, and Au–Ag–MoS_2 systems with and without the NO gas are shown in Fig. 7(a)-7(d). The figure reveals new peaks after adding NO, hence they are assigned to the gas. As shown in Fig. 7 (a), some new peaks appear in the range from 0.04 to 1.11 eV in the conduction band upon the adsorption of NO on the surface of MoS_2 indicating the decrease of its band gap. This result is in decent agreement with the band structures of NO/MoS_2 (Fig. 5(a)) in which, some

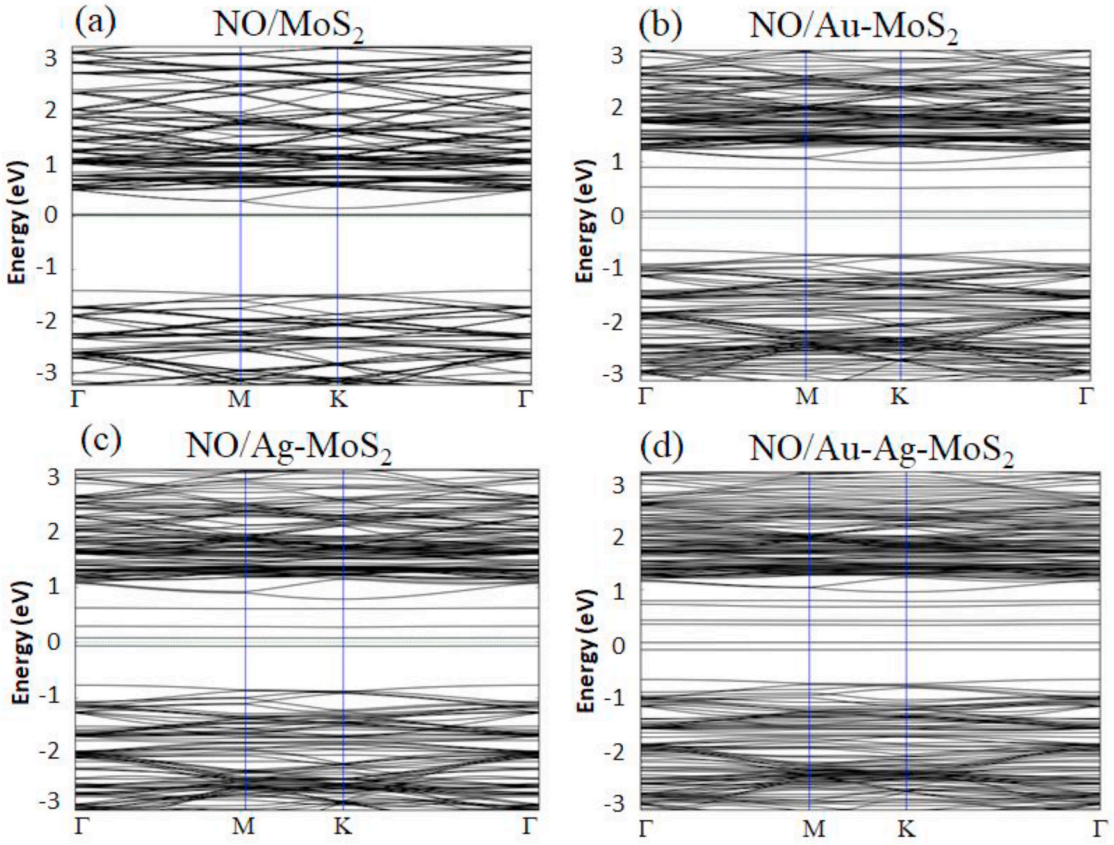

Fig. 5. Band structures of a) NO/MoS_2, b) $NO/Au–MoS_2$, c) $NO/Ag–MoS_2$, and d) $NO/Au–Ag–MoS_2$.

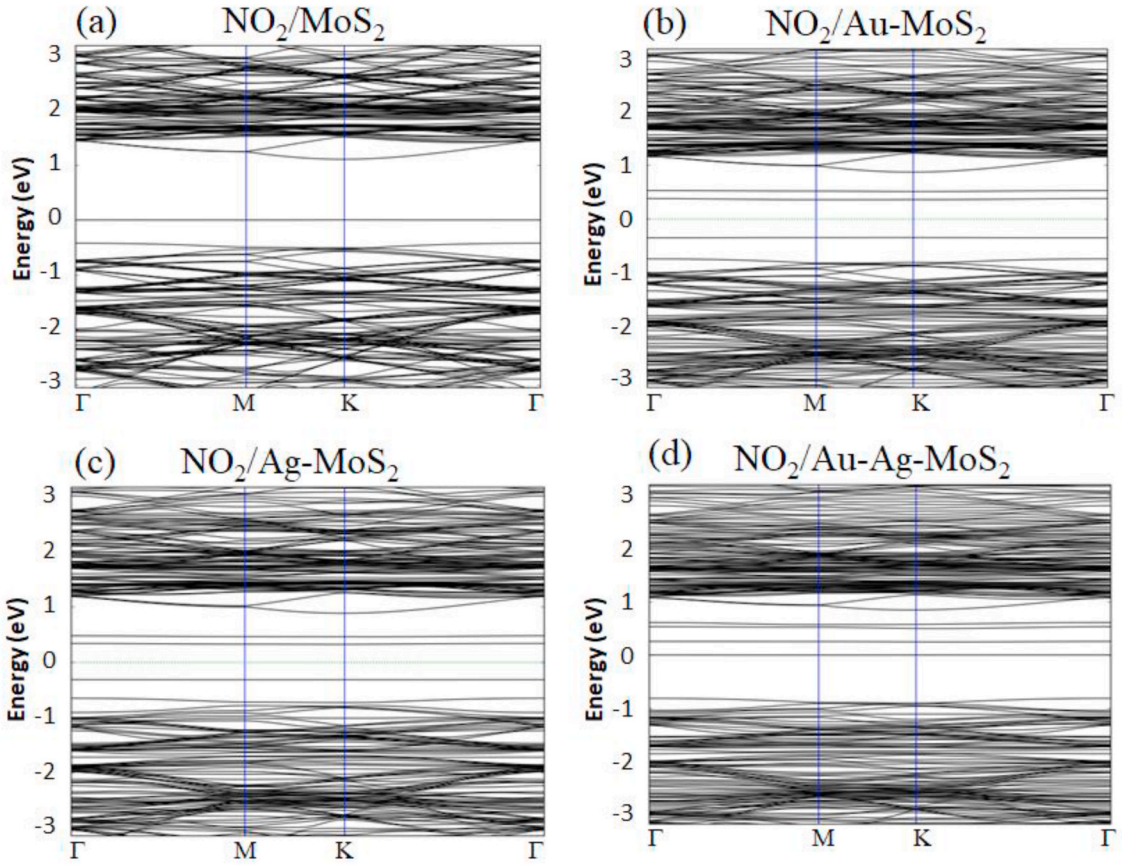

Fig. 6. Band structures of a) NO_2/MoS_2, b) $NO_2/Au–MoS_2$, c) $NO_2/Ag–MoS_2$, and d) $NO_2/Au–Ag–MoS_2$.

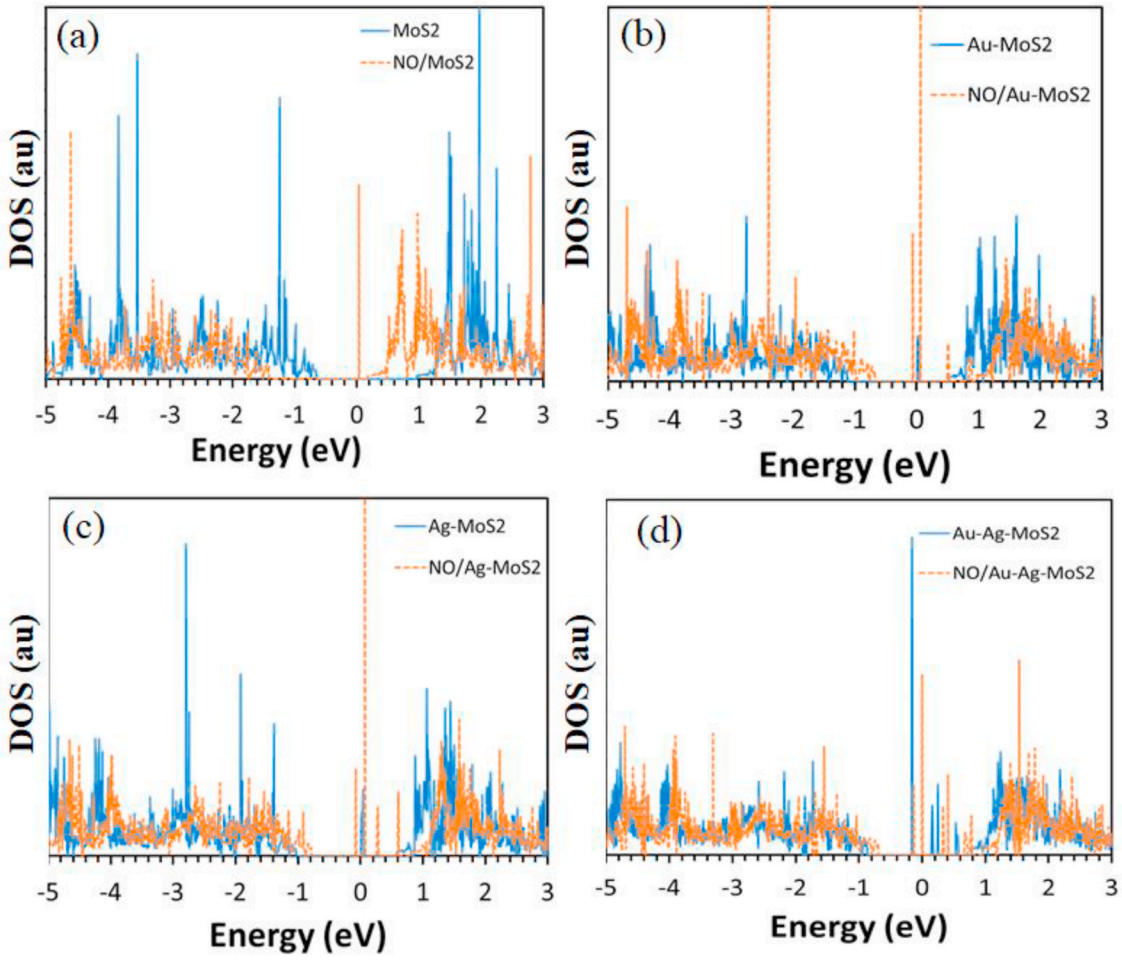

Fig. 7. Density of states, with and without NO, of a) MoS_2, b) Au–MoS_2, c) Ag–MoS_2, and d) Au–Ag–MoS_2.

new bands are detected in the same range after the adsorption of NO as compared with the pristine MoS_2. Meanwhile, remarkable variations in the intensity of the peaks in the ranges from 1.4 to 3.0 eV, −0.70 to −1.60, and −3.50 to −4.80 are observed due to gas adsorption. For the case of Au–MoS_2 shown in Fig. 7(b), the peaks at around −4.70, −2.40, and 0.06 eV increase significantly after the adsorption of NO. Moreover, a new peak is observed in the valence band close to the Fermi level at about −0.06 eV. The two peaks at −0.06 and 0.06 eV are represented by two bands close to the Fermi level in the band structures of NO/Au–MoS_2 (Fig. 5(b)). After the adsorption of NO on the surface of Ag–MoS_2 (Fig. 7(c)), the peak around 0.07 eV increases remarkably in addition to the appearance of new peaks around −0.92, −0.07, 0.26, and 0.61 eV. Furthermore, a new peak is detected at Fermi level upon the adsorption of NO on the surface of Au–Ag–MoS_2 (Fig. 7(d)) confirming the appearance of a new band at the same position in the band structure results of NO/Au–Ag–MoS_2 (Fig. 5(d)). The density of states of MoS_2, Au–MoS_2, Ag–MoS_2, and Au–Ag–MoS_2 systems with and without the NO_2 gas are shown in Fig. 8(a)–8(d). The figure reveals new peaks after adding NO_2, hence they are assigned to the gas. For the case of NO_2/MoS_2 (Fig. 8(a)), a new peak is detected at the Fermi level upon adsorption of the gas. While, the peak at around 0.02 eV of Au–MoS_2 disappear after the adsorption of NO_2 and new peaks around 0.36 eV, 0.51 eV, and in the range from −0.79 to 1.07 eV are observed as shown in Fig. 8(b). The same behavior is nearly observed after the adsorption of NO_2 on top of Ag–MoS_2 as shown in Fig. 8(c). After the adsorption of NO_2 on the surface of Au–Ag–MoS_2 (Fig. 8(d)), the two bands around −0.16 and 0.16 eV disappear and a new peak at Fermi level is observed which support the band structure results of NO_2/Au–Ag–MoS_2 (Fig. 6(c)). Additionally, the peaks around −4.71 and 1.31 eV increase considerably after the gas adsorption. The variations in the bandgap for MoS_2 are assigned to quantum confinement as well as changing the hybridization among d and s orbitals for molybdenum atoms as well as sulfur atoms, correspondingly. For the NO case, charge transfer to MoS_2, and the changes near Fermi level are mostly assigned to the p orbitals of N according to the DOS analysis. Adsorption of NO_2 gas on MoS_2 causes to the Fermi level to be down shifted to the valence band, representing hole doping of MoS_2. Remarkably, the substantial orbital hybridizations among both NO and NO_2 to the Au–MoS_2 system that are localized close the Fermi level in Figs. 4–6. For the NO case, the band structure reveals a nearly flat band corresponding with the NO spin states (up) near Fermi level that justifies its high sensitivity for NO adsorption. The variations that are demonstrated in the density of states of the proposed MoS_2, Au–MoS_2, Ag–MoS_2, and Au–Ag–MoS_2 systems upon the adsorption of both NO and NO_2 gases is a justification of the change in the occupied number of states of those systems [38]. These results prove that developed systems of the current study successfully adsorbed the target NO and NO_2 gases.

4. Conclusion

The current work is concerned of finding a sensitive gas sensor for the efficient detection of NO and NO_2 gases. Hence, doping and codoping was employed to generate four different molybdenum disulfide (MoS_2) based sensor materials that include: MoS_2, Au–MoS_2, Ag–MoS_2, and Au–Ag–MoS_2. The electronic characteristics as well as the adsorption capacity of the proposed sensor materials were investigated

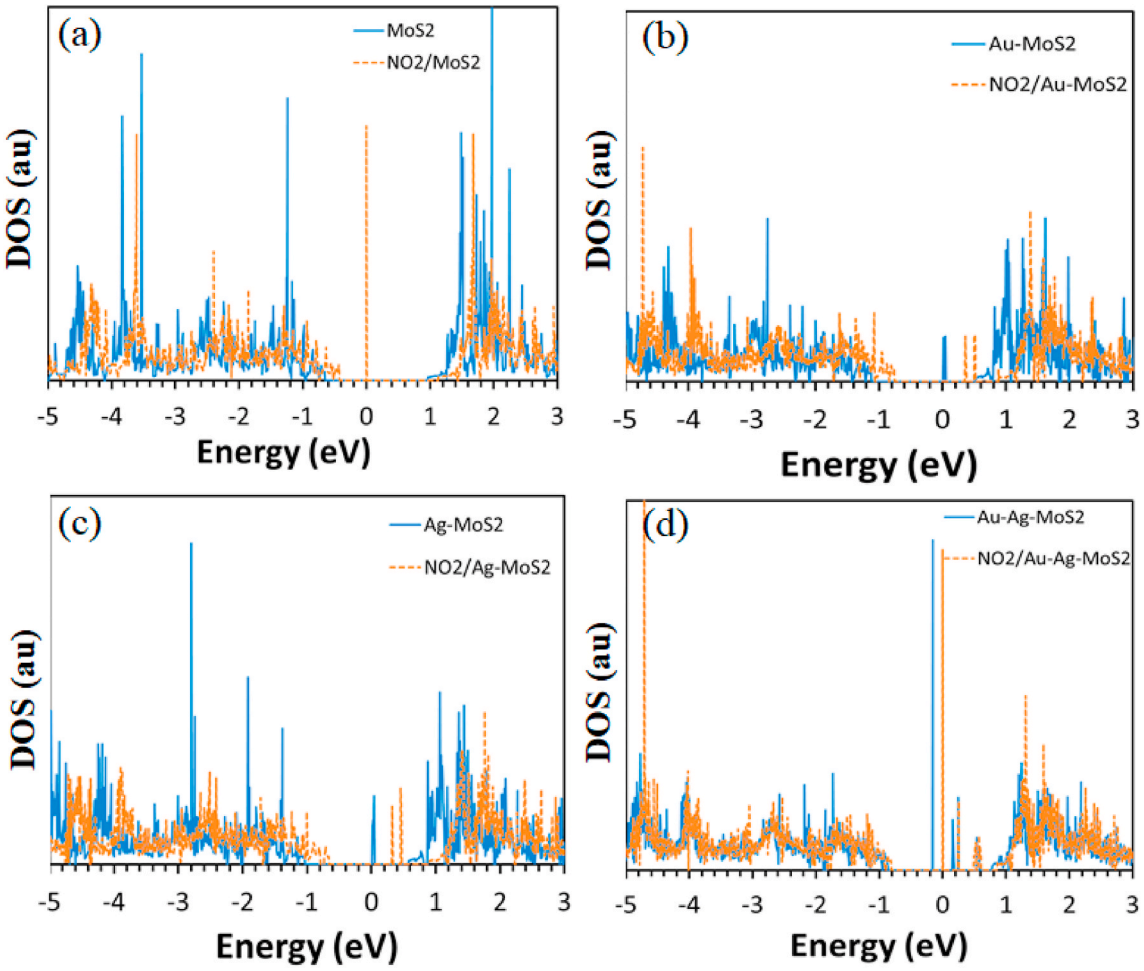

Fig. 8. Density of states, with and without NO_2, of a) MoS_2, b) Au–MoS_2, c) Ag–MoS_2, and d) Au–Ag–MoS_2.

based on DFT calculations. The results demonstrated significant changes in the electronic properties and adsorption parameters toward NO and NO_2 molecules upon the modification of MoS_2. For the case of NO gas, the highest adsorption energy of −0.721 eV was observed with Au–MoS_2 system. Therefore, this system is considered to be selective for NO. By comparing the two gases, the adsorption parameters were found to be considerably improved for the case of NO_2 gas. Specifically, the adsorption energy along with charge transfer increased remarkably to 16 times and 3 times, respectively, for the case of NO_2/Au–Ag–MoS_2 when compared with NO_2/MoS_2. Therefore, from the four systems the Au and Ag codoped-MoS_2 system is selective to NO_2 gas. The results obtained in this work indicate that Au and Ag codoped-MoS_2 can be considered as a sensitive gas sensor for NO_2 gas.

Declaration of competing interest

The authors declare that they have no known competing financial interests or personal relationships that could have appeared to influence the work reported in this paper.

Acknowledgements

The publication of this article was funded by the Qatar National Library.

References

[1] E. Salih, A.I. Ayesh, Enhancing the sensing performance of zigzag graphene nanoribbon to detect NO, NO2, and NH3 gases, Sensors 20 (2020) 3932.
[2] C.-T. Lee, H.-Y. Lee, Y.-S. Chiu, Performance improvement of nitrogen oxide gas sensors using Au catalytic metal on SnO 2/WO 3 complex nanoparticle sensing layer, IEEE Sensor. J. 16 (2016) 7581–7585.
[3] C. Di Natale, R. Paolesse, E. Martinelli, R. Capuano, Solid-state gas sensors for breath analysis: a review, Anal. Chim. Acta 824 (2014) 1–17.
[4] I.D. Pavord, D.E. Shaw, P.G. Gibson, D.R. Taylor, Inflammometry to assess airway diseases, Lancet 372 (2008) 1017–1019.
[5] B.T. Marquis, J.F. Vetelino, A semiconducting metal oxide sensor array for the detection of NOx and NH3, Sensor. Actuator. B Chem. 77 (2001) 100–110.
[6] H. Xia, Y. Wang, F. Kong, S. Wang, B. Zhu, X. Guo, J. Zhang, Y. Wang, S. Wu, Au-doped WO3-based sensor for NO2 detection at low operating temperature, Sensor. Actuator. B Chem. 134 (2008) 133–139.
[7] L. Yang, A. Marikutsa, M. Rumyantseva, E. Konstantinova, N. Khmelevsky, A. Gaskov, Quasi similar routes of NO2 and NO sensing by nanocrystalline WO3: evidence by in situ drift spectroscopy, Sensors 19 (2019) 3405.
[8] L. Guo, Y.-W. Hao, P.-L. Li, J.-F. Song, R.-Z. Yang, X.-Y. Fu, S.-Y. Xie, J. Zhao, Y.-L. Zhang, Improved NO 2 gas sensing properties of graphene oxide reduced by two-beam-laser interference, Sci. Rep. 8 (2018) 1–7.
[9] M. Chhowalla, H.S. Shin, G. Eda, L.-J. Li, K.P. Loh, H. Zhang, The chemistry of two-dimensional layered transition metal dichalcogenide nanosheets, Nat. Chem. 5 (2013) 263–275.
[10] S. Stankovich, D.A. Dikin, G.H. Dommett, K.M. Kohlhaas, E.J. Zimney, E.A. Stach, R.D. Piner, S.T. Nguyen, R.S. Ruoff, Graphene-based composite materials, Nature 442 (2006) 282–286.
[11] F.K. Perkins, A.L. Friedman, E. Cobas, P. Campbell, G. Jernigan, B.T. Jonker, Chemical vapor sensing with monolayer MoS2, Nano Lett. 13 (2013) 668–673.
[12] Q. He, Z. Zeng, Z. Yin, H. Li, S. Wu, X. Huang, H. Zhang, Fabrication of flexible MoS2 thin-film transistor arrays for practical gas-sensing applications, Small 8 (2012) 2994–2999.

[13] R.V. Poonguzhali, E. Ranjith Kumar, T. Pushpagiri, A. Steephen, N. Arunadevi, S. Baskoutas, Lemon juice (natural fuel) assisted synthesis of MgO nanorods for LPG gas sensor applications, Solid State Commun. 325 (2021) 114161.
[14] M. D, S. Ch, E. R K, R. P N, N.K. Mohan, M. Sher Singh, C.L. Prajapat, A. Verma, D. L. Sastry, Evaluation of structural and dielectric properties of Mn2+-substituted Zn-spinel ferrite nanoparticles for gas sensor applications, Sensor. Actuator. B Chem. 316 (2020) 128127.
[15] K.F. Mak, C. Lee, J. Hone, J. Shan, T.F. Heinz, Atomically thin MoS 2: a new direct-gap semiconductor, Phys. Rev. Lett. 105 (2010) 136805.
[16] J. Zhu, H. Zhang, Y. Tong, L. Zhao, Y. Zhang, Y. Qiu, X. Lin, First-principles investigations of metal (V, Nb, Ta)-doped monolayer MoS2: structural stability, electronic properties and adsorption of gas molecules, Appl. Surf. Sci. 419 (2017) 522–530.
[17] Z. Xiao, W. Wu, X. Wu, Y. Zhang, Adsorption of NO2 on monolayer MoS2 doped with Fe, Co, and Ni, Cu: a computational investigation, Chem. Phys. Lett. 755 (2020) 137768.
[18] J. Wang, Q. Zhou, L. Xu, X. Gao, W. Zeng, Gas sensing mechanism of dissolved gases in transformer oil on Ag–MoS2 monolayer: a DFT study, Phys. E Low-dimens. Syst. Nanostruct. 118 (2020) 113947.
[19] T. Pham, G. Li, E. Bekyarova, M.E. Itkis, A. Mulchandani, MoS2-Based Optoelectronic gas sensor with sub-parts-per-billion limit of NO2 gas detection, ACS Nano 13 (2019) 3196–3205.
[20] D. Ma, W. Ju, T. Li, X. Zhang, C. He, B. Ma, Z. Lu, Z. Yang, The adsorption of CO and NO on the MoS2 monolayer doped with Au, Pt, Pd, or Ni: a first-principles study, Appl. Surf. Sci. 383 (2016) 98–105.
[21] J.P. Perdew, K. Burke, M. Ernzerhof, Generalized gradient approximation made simple, Phys. Rev. Lett. 77 (1996) 3865.
[22] S. Grimme, Semiempirical GGA-type density functional constructed with a long-range dispersion correction, J. Comput. Chem. 27 (2006) 1787–1799.
[23] D. Liu, Y. Gui, C. Ji, C. Tang, Q. Zhou, J. Li, X. Zhang, Adsorption of SF6 decomposition components over Pd (1 1 1): a density functional theory study, Appl. Surf. Sci. 465 (2019) 172–179.
[24] E. Salih, A.I. Ayesh, CO, CO2, and SO2 detection based on functionalized graphene nanoribbons: first principles study, Phys. E Low-dimens. Syst. Nanostruct. (2020) 114220.
[25] E. Salih, A.I. Ayesh, First principle investigation of H2Se, H2Te and PH3 sensing based on graphene oxide, Phys. Lett. 384 (2020) 126775.
[26] R.S. Mulliken, Electronic population analysis on LCAO–MO molecular wave functions. I, J. Chem. Phys. 23 (1955) 1833–1840.
[27] T. Pakornchote, A. Ektarawong, B. Alling, U. Pinsook, S. Tancharakorn, W. Busayaporn, T. Bovornratanaraks, Phase stabilities and vibrational analysis of hydrogenated diamondized bilayer graphenes: a first principles investigation, Carbon 146 (2019) 468–475.
[28] M.G. Ahangari, A.H. Mashhadzadeh, M. Fathalian, A. Dadrasi, Y. Rostamiyan, A. Mallahi, Effect of various defects on mechanical and electronic properties of zinc-oxide graphene-like structure: a DFT study, Vacuum 165 (2019) 26–34.
[29] X. Gao, Q. Zhou, J. Wang, L. Xu, W. Zeng, Adsorption of SO2 molecule on Ni-doped and Pd-doped graphene based on first-principle study, Appl. Surf. Sci. (2020) 146180.
[30] B. Zhao, C. Li, L. Liu, B. Zhou, Q. Zhang, Z. Chen, Z. Tang, Adsorption of gas molecules on Cu impurities embedded monolayer MoS2: a first-principles study, Appl. Surf. Sci. 382 (2016) 280–287.
[31] M.P.K. Sahoo, J. Wang, Y. Zhang, T. Shimada, T. Kitamura, Modulation of gas adsorption and magnetic properties of monolayer-MoS2 by antisite defect and strain, J. Phys. Chem. C 120 (2016) 14113–14121.
[32] D. Ma, W. Ju, T. Li, X. Zhang, C. He, B. Ma, Y. Tang, Z. Lu, Z. Yang, Modulating electronic, magnetic and chemical properties of MoS2 monolayer sheets by substitutional doping with transition metals, Appl. Surf. Sci. 364 (2016) 181–189.
[33] M. Donarelli, S. Prezioso, F. Perrozzi, F. Bisti, M. Nardone, L. Giancaterini, C. Cantalini, L. Ottaviano, Response to NO2 and other gases of resistive chemically exfoliated MoS2-based gas sensors, Sensor. Actuator. B Chem. 207 (2015) 602–613.
[34] K. Kam, B. Parkinson, Detailed photocurrent spectroscopy of the semiconducting group VIB transition metal dichalcogenides, J. Phys. Chem. 86 (1982) 463–467.
[35] A. Kuc, N. Zibouche, T. Heine, Influence of quantum confinement on the electronic structure of the transition metal sulfide T S 2, Phys. Rev. B 83 (2011) 245213.
[36] X. Deng, X. Liang, S.-P. Ng, C.-M.L. Wu, Adsorption of formaldehyde on transition metal doped monolayer MoS2: a DFT study, Appl. Surf. Sci. 484 (2019) 1244–1252.
[37] V.E.C. Padilla, M.T.R. de la Cruz, Y.E.Á. Alvarado, R.G. Díaz, C.E.R. García, G. H. Cocoletzi, Studies of hydrogen sulfide and ammonia adsorption on P-and Si-doped graphene: density functional theory calculations, J. Mol. Model. 25 (2019) 94.
[38] G.K. Walia, D.K.K. Randhawa, First-principles investigation on defect-induced silicene nanoribbons—a superior media for sensing NH3, NO2 and NO gas molecules, Surf. Sci. 670 (2018) 33–43.